

# Successive common envelope events from multiple planets

Luke Chamandy,<sup>1\*</sup> Eric G. Blackman,<sup>1†</sup> Jason Nordhaus<sup>2,3‡</sup> and Emily Wilson<sup>2§</sup>

<sup>1</sup>*Department of Physics and Astronomy, University of Rochester, Rochester NY 14627, USA*

<sup>2</sup>*Center for Computational Relativity and Gravitation, Rochester Institute of Technology, Rochester, NY 14623, USA*

<sup>3</sup>*National Technical Institute for the Deaf, Rochester Institute of Technology, Rochester, NY 14623, USA*

22nd December 2024

## ABSTRACT

Many stars harbour multi-planet systems. As these stars expand late in their evolutions, the innermost planet may be engulfed, leading to a common envelope (CE) event. Even if this is insufficient to eject the envelope, it may expand the star further, causing additional CE events, with the last one unbinding what remains of the envelope. This multi-planet CE scenario may have broad implications for stellar and planetary evolution across a range of systems. We develop a simplified version and show that it may be able to explain the recently observed planet WD 1856 b.

**Key words:** planetary systems: formation – white dwarfs – stars: AGB and post-AGB – binaries: close

## 1 INTRODUCTION

Vanderburg et al. (2020) (hereafter V20) recently detected the Jupiter-sized object WD 1856 b orbiting a white dwarf (WD) with orbital period 1.4d. They calculated the WD mass to be  $(0.518 \pm 0.055) M_{\odot}$ , and obtained an upper limit of  $13.8 M_{\text{J}}$  implying that it is likely a planet. The semi-major axis of  $\sim 4 R_{\odot}$  places it well within the envelope of the progenitor star, but inside of the WD-planet period gap predicted by Nordhaus et al. (2010).<sup>1</sup> A single common envelope (CE) event origin is thus unlikely (Nordhaus & Spiegel 2013). Likewise, V20 found that a single CE origin is unlikely. Lagos et al. (2021) argued that a single CE origin is not ruled out if energy additional to the released orbital energy contributes to envelope unbinding. They also argue that a CE scenario is consistent with the youth needed to account for apparent membership in the Galactic thin disc.

Using Modules for Experiments in Stellar Astrophysics (MESA) (Paxton et al. 2019), we also assessed the single CE scenario based on detailed stellar interior models which match the initial-final mass relation (Cummings et al. 2018). Assuming that orbital energy alone is used to eject the envelope with maximum efficiency Wilson & Nordhaus 2019, 2020 we find that the stellar envelope around a WD core of mass  $(0.518 \pm 0.055) M_{\odot}$  can be ejected by a companion of  $13.8 M_{\text{J}}$  or less only if the initial primary mass is  $< 1.2 M_{\odot}$ . Successful single CE scenarios resulting in the observed 1.4d period can only occur during the late stages of the asymptotic giant branch (AGB) phase with  $< 0.1 M_{\odot}$  left in the envelope and average envelope-mass-to-core-mass ratio  $< 0.14$ . But for

this stellar mass range, the CE would initiate on the red giant branch (RGB), leaving a WD of too little mass. This system is thus unlikely the result of a single CE interaction.

V20 consider ideas other than CE to explain the orbit of WD 1856 b, and favour planet migration from a larger orbit by the von Zeipel-Lidov-Kozai (ZLK) effect (von Zeipel 1910; Lidov 1962; Kozai 1962) in tandem with tidal friction (Wu & Murray 2003; Fabrycky & Tremaine 2007). They conclude that WD 1856 b’s M-dwarf companions G 229-20 A/B were unlikely to have triggered the migration, but that unseen planets could have done so. By contrast, Muñoz & Petrovich (2020), O’Connor et al. (2021) and Stephan et al. (2020) find regions of parameter space for which the M-dwarf companions can excite the ZLK effect, but disagree on the importance of various terms and the initial semi-major axis of WD 1856 b.

WD J0914 may also host a planet (Gänsicke et al. 2019), as inferred by modeling observational signatures of accretion. The cooling age of WD J0914 is only  $\sim 13$  Myr, leaving little time for migration to its present orbit of semi-major axis  $\sim 15 R_{\odot}$ . The ZLK-tidal friction mechanism is a possible explanation, but it may require the presence of an unseen companion with mass  $\gtrsim 0.3 M_{\odot}$  (Stephan et al. 2020). A single CE origin may be possible if the planet mass  $\gtrsim 1 M_{\text{J}}$ , but the mass may be smaller (Gänsicke et al. 2019).

Here we devise a model that involves successive planet-induced CE events to explain WD 1856 b. Such a scenario was mentioned by Nordhaus et al. (2010), and Lagos et al. (2021) in the context of WD 1856 b, but has not yet been quantified. Here we demonstrate that such a model is efficacious. We focus on WD 1856, but the model can be applied to other systems such as WD J0914. The scenario starts with a CE interaction involving planet 1 – which is subsequently tidally disrupted – and the post-main sequence WD progenitor. Different pathways to the first CE (CE1) (e.g. Villaver & Livio 2009; Chen et al. 2018; MacLeod et al. 2018) apply to planet 1, but subsequent rapid expansion of the primary engulfs the wider orbit of planet-2, causing a second CE (CE2).

\* lchamandy@pas.rochester.edu

† blackman@pas.rochester.edu

‡ nordhaus@astro.rit.edu

§ ecw7497@rit.edu

<sup>1</sup> The WD-planet period gap is the orbital region around a WD that is predicted to be devoid of planets due to previous interactions during stellar evolution.

We assume that CE1 and CE2 combine to remove the envelope, and planet 2 survives in orbit.<sup>2</sup>

The observed mass of WD 1856 constrains the zero-age main sequence mass of its progenitor,  $M_0$ . For  $M_0 \lesssim 1.0 M_\odot$ , the maximum RGB radius exceeds that of the AGB, so CE will occur on the RGB, and leave too small of a WD core. For  $M_0 \gtrsim 3.5 M_\odot$ , the core is too massive on the AGB, but, coincidentally, attains high enough mass on the RGB. But a high mass star, higher envelope binding energy, and smaller RGB vs. AGB radius make CE in this mass range less likely. For  $1.0 \lesssim M_0/M_\odot \lesssim 3.5$ , CE likely occurs on the AGB with a core mass  $M_{\text{wd}} = (0.518 \pm 0.055) M_\odot$ . We expect CE to occur before the AGB tip. There, a  $1 M_\odot$  star has lost  $\sim 0.4 M_\odot$ , and a  $3.5 M_\odot$  star has lost little before the start of the AGB. Therefore, the AGB mass before CE1 is  $0.6 \lesssim M_1/M_\odot \lesssim 3.5$ .

In Sec. 2, we compute the respective fractions of the initial envelope binding energy injected during CE2 and CE1 for a given mass  $m_2$  of planet 2. We then determine the mass  $m_1$  of planet 1, for limiting cases to bracket its range. For plausible models, CE1 should cause CE2. We estimate the expansion of the star during CE1, and show that it can be large enough for the star to engulf the second, more distant planet 2. In Sec. 3, we incorporate radiative cooling.

## 2 TWO-PLANET CE SCENARIO

### 2.1 Planet mass combinations for two limiting cases

To exemplify, we use the WD mass, radius, and planet 2 orbital radius or V20:  $M_{\text{wd}} = 0.518 M_\odot$ ,  $R_{\text{wd}} = 1.31 \times 10^{-2} R_\odot$ , and  $P_2 = 1.408$  d. Subscript ‘1’ and ‘2’ will delineate the state of the system at the start of CE1 and CE2 respectively. Each planet mass is assumed constant, but we allow tidal disruption of planet 1. The binding energy (defined  $> 0$ ) of the envelope at the start of mass transfer that leads to CE1 is

$$E_1 = \frac{GM_1 M_{e,1}}{\lambda_1 R_1}, \quad (1)$$

where  $G$  is the gravitational constant,  $M_1$  and  $M_{e,1}$  are the original masses of the primary and envelope;  $R_1$  is the original radius of the primary; and  $\lambda_1$  is a conventional dimensionless parameter accounting for distinct radial energy profiles. If a fraction  $\beta_1$  of the energy needed to unbind the envelope is supplied by CE1, then CE2 need supply only a fraction  $\beta_2 = 1 - \beta_1$  to unbind the remaining envelope. The CE energy formalism (e.g. Ivanova et al. 2013) applied to CE1 then gives

$$\beta_1 E_1 = (1 - \beta_2) E_1 \simeq \alpha_1 \frac{GM_{\text{wd}} m_1}{2a_{f,1}}, \quad (2)$$

where  $\alpha_1$  is a conventional dimensionless parameter accounting for the energy conversion efficiency of the unbinding,  $m_1$  is the mass of planet 1, the primary core mass is assumed equal to  $M_{\text{wd}}$ ,  $a_{f,1}$  is the binary separation at the end of CE1, the small mass of the envelope interior to the orbit has been neglected (or can be absorbed into the factor  $\beta_1$ ), and the term  $-\alpha_1 GM_1 m_1 / 2a_{i,1}$  on the right side (with  $a_{i,1}$  the initial separation) is neglected as in V20; we have checked that this term is generally small. Similarly, for CE2

$$\beta_2 E_1 \simeq \alpha_2 \frac{GM_{\text{wd}} m_2}{2a_{f,2}}. \quad (3)$$

Dividing equation (2) by equation (3), and rearranging gives

$$m_1 = \frac{a_{f,1} \alpha_2}{a_{f,2} \alpha_1} \left( \frac{1}{\beta_2} - 1 \right) m_2. \quad (4)$$

V20 constrained  $m_2 \leq 14 M_J$ , though it is not precisely known. Dividing equation (3) by equation (1) gives

$$\beta_2 = \frac{M_{\text{wd}} m_2}{2(M_1 - M_{\text{wd}}) M_1} \frac{\alpha_1 \lambda_1 R_1}{a_{f,2}} \frac{\alpha_2}{\alpha_1}, \quad (5)$$

where we have substituted  $M_{e,1} = M_1 - M_{\text{wd}}$ . The quantity  $a_{f,2}$  is related to the observed period by Kepler’s third law:

$$a_{f,2} = \left[ G(M_{\text{wd}} + m_2) \left( \frac{P_{f,2}}{2\pi} \right)^2 \right]^{1/3} \simeq \left( \frac{GM_{\text{wd}} P_{f,2}^2}{4\pi^2} \right)^{1/3}, \quad (6)$$

where  $P_{f,2} = 1.4$  d is the observed period. In the rightmost expression and below, we assume  $m_1, m_2 \ll M_{\text{wd}}$ .

In the top panel of Fig. 1 we plot  $\beta_2$  against  $m_2$ , in Jupiter masses, for various values of  $\alpha_1 \lambda_1$  chosen to be consistent with estimates of V20, for either  $M_1 = 1 M_\odot$  or  $M_1 = 3 M_\odot$ . Since  $\beta_2 < 1$  for  $m_2 < 14 M_J$ , a single CE scenario fails, in agreement with V20. On the other hand, extremely small values of  $\beta_2$  would require fine-tuning  $\beta_1$  to be just less than 1. We see that  $\beta_2$  can take on values up to 0.15 for  $m_2 < 14 M_\odot$ . Focusing on  $\beta_2 > 0.01$  gives  $\alpha_1 \lambda_1 \gtrsim 0.4$  in the  $3 M_\odot$  model and also determines a corresponding lower limit on  $m_2$ .

Following V20, we assume  $R_1$  to be equal to the primary’s Roche lobe when mass transfer initiates, and then make use of their fitting formula for  $R_1$  in terms of  $M_{\text{wd}}$ . This gives

$$R_1 = 5.56 \times 10^4 f(M_{\text{wd}}/M_\odot) R_\odot, \quad (7)$$

where  $f(\mu) \equiv \mu^{19/3} / (1 + 20\mu^3 + 10\mu^6) + f_0$ , with  $f_0 = 7.2 \times 10^{-5}$ .

For  $a_{f,1}$ , we consider two limiting cases: (i) the planet merges with the WD, with all of the liberated orbital energy released to the envelope so

$$a_{f,1} \simeq R_{\text{wd}} \approx 1.3 \times 10^{-2} R_\odot \quad (\text{case i}), \quad (8)$$

and (ii) after the planet gets tidally disrupted, its orbital energy is no longer used to unbind the envelope. In this case, we can estimate (c.f. Nordhaus & Blackman 2006)

$$\begin{aligned} a_{f,1} &= a_{d,1} \simeq \left( \frac{2M_{\text{wd}}}{m_1} \right)^{1/3} r_1 \quad (\text{case ii}) \\ &\simeq 1.0 R_\odot \left( \frac{M_{\text{wd}}}{0.52 M_\odot} \right)^{1/3} \left( \frac{m_1}{10^{-3} M_\odot} \right)^{-1/3} \left( \frac{r_1}{0.1 R_\odot} \right), \end{aligned} \quad (9)$$

where  $a_{d,1}$  is the tidal disruption radius, measured from the centre of the primary’s core, and  $r_1$  is the radius of planet 1. Cases (i) and (ii) bracket the range of possibilities.

Equation (4), with equations (5), (6), (7), and (8) or (9), are then used to obtain  $m_1$  in terms of  $\alpha_1 \lambda_1$ ,  $a_{f,1}$ ,  $m_2$ ,  $P_{f,2}$ ,  $M_{\text{wd}}$ ,  $M_1$  and the ratio  $\alpha_2/\alpha_1$ . The results are plotted in the bottom panel of Fig. 1, for  $\alpha_1/\alpha_2 = 1$  and the parameter values mentioned in the figure legend and caption. Case (i),  $a_{f,1} = R_{\text{wd}}$ , is represented by thick lines, and thin lines show case (ii),  $a_{f,1} = a_{d,1}$ , assuming  $r_1 = 0.1 R_\odot$ . For  $M_1 = 1 M_\odot$ , we see that the required planet mass needed to inject the fraction  $\beta_1$  of the original envelope binding energy falls within a reasonable range of  $0.2 \lesssim m_1/M_J \lesssim 30$ . For  $M_1 = 3 M_\odot$  we obtain  $0.3 \lesssim m_1/M_J \lesssim 5$  if  $a_{f,1} = R_{\text{wd}}$ , but  $10 \lesssim m_1/M_J \lesssim 80$  if  $a_{f,1} = a_{d,1}$  is adopted. The latter range falls mostly above the usual planet-brown dwarf boundary of  $\sim 13 M_J$ .

Fig. 1 shows that there is a large section of parameter

<sup>2</sup> The scenario can be generalized for more planets.

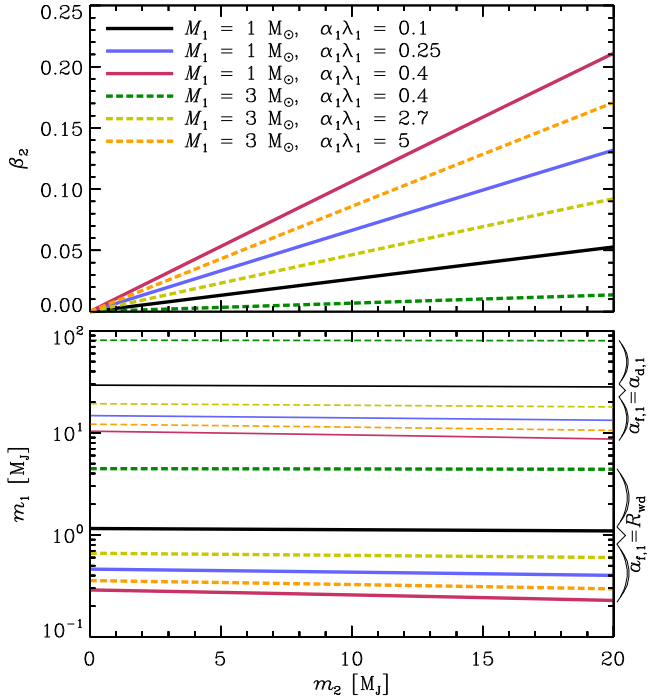


**Figure 1.** *Top:* The fraction  $\beta_2$  of the original binding energy  $E_1$  injected during CE2, versus the mass of planet 2. *Bottom:* The mass  $m_1$  of planet 1 required to inject the fraction  $\beta_1 = 1 - \beta_2$  of the binding energy  $E_1$ , assuming that the final separation is equal to the WD radius,  $a_{f,1} = R_{\text{wd}}$  (thick lines), or to the tidal disruption separation,  $a_{f,1} = a_{d,1}$  (thin lines). The latter is calculated assuming that the planet radius  $r_1 = 0.1 R_{\odot}$ . The lines are not exactly horizontal. In both panels  $\alpha_1/\alpha_2 = 1$  is used. V20 constrain the mass of WD 1856 b to be  $0.1 \leq m_2/M_{\text{J}} \leq 13.8$ .

space that produces  $\beta_2 > 0.01$  and realistic values for  $m_1$ , viz.  $0.2 \leq m_1/M_{\text{J}} \lesssim 30$ . The smaller value of  $M_1 = 1 M_{\odot}$  (solid lines) leads to a larger viable parameter space than with  $M_1 = 3 M_{\odot}$  (dashed lines). The  $1 M_{\odot}$  value may be favoured because the initial mass function is weighted toward lower-mass progenitors (Chabrier 2003).

## 2.2 Expansion of the envelope during CE1

While it is possible that the primary star could expand on its canonical evolutionary time ( $\gtrsim$  Myr) to eventually engulf planet 2, this time is much longer than typical CE plunge times of days to years (e.g. Chamandy et al. 2020). Here we explain why planet 2 could be engulfed as a *result* of CE1.

During CE1, energy is predominantly deposited at the base of the envelope, due to the  $1/r$  potential and centrally condensed evolved star. We expect the envelope to respond by expanding. To estimate the expansion, we equate the initial energy just after CE1 with the final energy after the envelope has adjusted. The envelope might oscillate (Clayton et al. 2017), but we are only interested in the maximum radius reached. We also neglect any recombination energy release during expansion. We do not include a bulk kinetic energy term for the bound envelope but allow for escaping winds. We also do not consider the consequences of accretion for

nuclear fusion (Siess & Livio 1999a,b).<sup>3</sup> We obtain

$$-(1 - \beta_1) \frac{GM_1 M_{e,1}}{\lambda_1 R_1} = -\frac{GM_2 M_{e,2}}{\lambda_2 R_2} + E_{\text{ej}}. \quad (10)$$

where  $E_{\text{ej}}$  is the energy of the ejecta (wind), which is not well constrained. If the ejecta leaves at the escape speed, it will remove only a net thermal energy, as bulk kinetic and potential energies sum to zero. For convenience, we write

$$E_{\text{ej}} = \frac{1}{2} C' \frac{M_{\text{ej}} v_{\text{esc},2}^2}{\lambda_2} = \frac{C' GM_2 (M_{e,1} - M_{e,2})}{\lambda_2 R_2}, \quad (11)$$

with  $M_{\text{ej}} = M_{e,1} - M_{e,2}$  the ejecta mass,  $v_{\text{esc},2}$  the escape speed from the stellar surface in its final state, and  $C'$  a dimensionless constant of order unity. Substituting equation (11) into equation (10), and defining  $\lambda'_2 \equiv \lambda_2 M_{e,2} / (M_{e,2} - C' M_{\text{ej}})$ , the right of equation (10) becomes  $-GM_2 M_{e,2} / \lambda'_2 R_2$ . Note that  $\lambda'_2 \rightarrow \lambda_2$  as  $C' \rightarrow 0$  or  $E_{\text{ej}} \rightarrow 0$ . Rearranging equation (10) gives

$$\frac{R_2}{R_1} = \frac{1}{\beta_2} \frac{\lambda_1 M_2 M_{e,2}}{\lambda'_2 M_1 M_{e,1}}. \quad (12)$$

The mass of the ejecta  $M_{\text{ej}}$  cannot exceed  $M_{e,1} / (1 + C')$  or else  $R_2$  reduces to zero; we focus on solutions for which  $R_2 > R_1$ , which requires  $M_{\text{ej}}$  to be less than some smaller critical value. If  $M_{\text{ej}} = 0$ , then  $M_{e,2} = M_{e,1}$  and the solution reduces to

$$\frac{R_2}{R_1} = \frac{1}{\beta_2} \frac{\lambda_1}{\lambda_2}; \quad (\text{no mass loss}). \quad (13)$$

As example I, we take  $M_1 = 1 M_{\odot}$  so that  $M_{e,1} = M_1 - M_{\text{wd}} \approx 0.48 M_{\odot}$ , and adopt  $\lambda_1 = \lambda_2$ ,  $C' = 1$ , and  $\beta_2 = 0.1$ . Assuming no mass loss, we obtain  $R_2 = 10 R_1$ . The maximum ejecta mass ( $R_2 = 0$ ) is  $\approx 0.24 M_{\odot}$ , whilst  $R_2 = R_1$  for  $M_{\text{ej}} \approx 0.21 M_{\odot}$ . If  $M_{\text{ej}} = 0.1 M_{\odot}$ , we obtain  $R_2 = 5.3 R_1$ . As example II, we take  $M_1 = 3 M_{\odot}$ , which gives  $M_{e,1} \approx 2.48 M_{\odot}$ , and choose  $\lambda_2 = 3 \lambda_1$  (c.f. Xu & Li 2010),  $C' = 3$ , and  $M_{\text{ej}} = 0.3 M_{\odot}$ . Then we obtain  $R_2 = 1.5 R_1$ . For  $M_{\text{ej}} = 0$ , we obtain  $R_2 = 3.3 R_1$ . This exemplifies cases where the envelope expands enough to engulf a second planet.

The maximum expansion of the primary during CE1 constrains the maximum initial orbital radius of planet 2 to be engulfed. For small orbital eccentricities and stellar mass loss, mutual planet-planet perturbations are not expected to greatly restrict the mutual proximity of the planets (Hill 1886; Debes & Sigurdsson 2002; Maldonado et al. 2020). However, assuming that  $a_{i,2} > a_{i,1}$ , CE1 requires  $a_{i,1} < R_2$ . Villaver & Livio (2009) determine the *maximum*  $a_{i,1}$  that still allows CE during the RGB for a Jupiter-mass planet with different primary masses (neglecting other planet influences). For  $M_1 = 1 M_{\odot}$  and  $3 M_{\odot}$ , they obtain  $\max(a_{i,1})/R_1 \approx 2.5$  and 1.2, respectively. Values of  $R_2/R_1$  from our model comfortably exceed these requirements. We do not include increases in  $a_{i,2}$  from mass loss (e.g. Veras et al. 2011) and decreases associated from consequent drag on planet 2.

## 3 ROLE OF COOLING

### 3.1 Expansion including cooling

Not all of the energy injected into the envelope during the CE phase contributes to unbinding it. This includes, but is

<sup>3</sup> Fusion releasing a fraction  $f$  of rest energy can energize more than accretion if  $\gtrsim GM_{\text{wd}} / (f R_{\text{wd}})$  of accreted mass fuses.

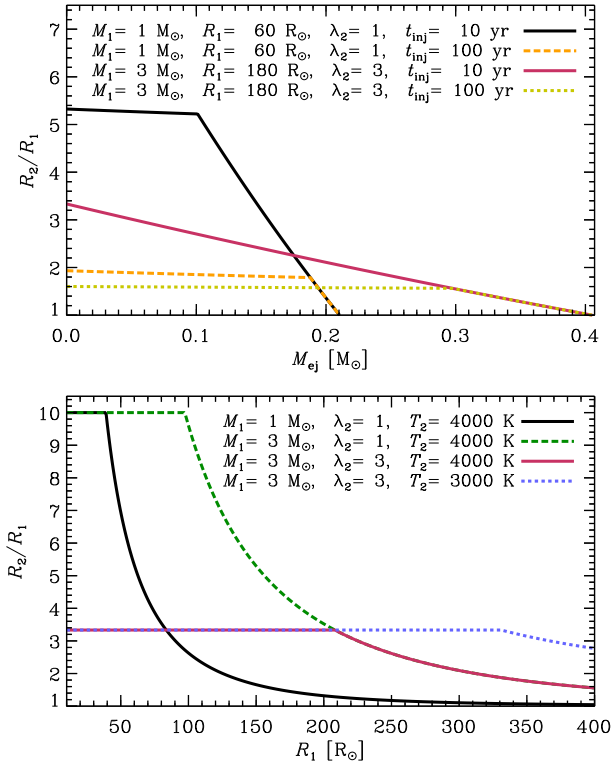


**Figure 2.** *Top:* The ratio  $R_2/R_1$  of the stellar radius before and after CE1 (which occurs on the AGB), as a function of the ejecta mass  $M_{\text{ej}}$ , with  $R_2$  calculated from equation (14). The steeper part of each curve corresponds to  $R_2 = R_{2,\text{max}}$ , obtained when cooling is neglected, i.e. when  $t_{\text{thm}} > t_{\text{inj}}$  in our model. If  $t_{\text{thm}} = t_{\text{inj}}$ , then  $R_2 = R_{2,\text{thm}}$ . All models have  $\beta_1 = 0.9$ ,  $\lambda_1 = 1$ ,  $C' = \lambda_2$ , and  $T_1 = T_2 = 4 \times 10^3$  K. *Bottom:* The ratio  $R_2/R_1$  plotted against the original radius  $R_1$ , for the case  $M_{\text{ej}} = 0$ , assuming  $\beta_1 = 0.9$ ,  $\lambda_1 = 1$ ,  $C' = \lambda_2$ ,  $T_1 = 4 \times 10^3$  K, and  $t_{\text{inj}} = 10$  yr. Wherever  $t_{\text{thm}} > t_{\text{inj}}$ ,  $R_2/R_1$  is independent of  $R_1$  and the curve is flat.

not limited to, energy lost via radiation that would have otherwise assisted unbinding. This is among the inefficiencies included in the  $\alpha$ -parameter of equations (2) and (3).

However, if cooling is as fast as energy injection, a “self-regulated” state could arise with the energy injected swiftly radiated (Meyer & Meyer-Hofmeister 1979; Ivanova et al. 2013), and the expansion of CE1 quenched. Here we modify the calculation of Sec. 2.2 to account for this.

We postulate that with cooling, either the star expands until it reaches the radius calculated in Sec. 2.2 or until the energy loss and injection rates balance. Thus,

$$R_2 = \min(R_{2,\text{thm}}, R_{2,\text{max}}), \quad (14)$$

where  $R_{2,\text{max}}$  is the value of  $R_2$  calculated in Sec. 2.2, and  $R_{2,\text{thm}}$  is estimated by equating the mean rates of energy injection and loss due to radiative cooling and winds, namely

$$\beta_1 \frac{GM_1 M_{\text{ej},1}}{\lambda_1 R_1 t_{\text{inj}}} \sim 4\pi\sigma(R_{2,\text{thm}}^2 T_2^4 - R_1^2 T_1^4) + \frac{C' GM_2 M_{\text{ej}}}{\lambda_2 R_{2,\text{thm}} t_{\text{inj}}}, \quad (15)$$

where  $t_{\text{inj}}$  is the energy injection time during CE1, (see Sec. 3.2); the left side is the energy injection rate  $E_{\text{inj}}/t_{\text{inj}}$ ; the first term on the right is the luminosity change  $\Delta L$ ;  $T_1$  and  $T_2$  are the effective temperatures of the star before and after CE1; and the last term is the rate of energy transfer to ejecta,

$E_{\text{ej}}/t_{\text{inj}}$ . The quantity  $R_2$  transitions from  $R_{2,\text{thm}}$  to  $R_{2,\text{max}}$  when  $t_{\text{inj}}$  falls below the cooling time  $t_{\text{thm}} = (E_{\text{inj}} - E_{\text{ej}})/\Delta L$ . Equation (15) reduces to a cubic in  $R_{2,\text{thm}}$ ,

$$R_{2,\text{thm}}^3 + bR_{2,\text{thm}} + c \sim 0, \quad (16)$$

where

$$b = - \left[ \frac{\beta_1 A M_1 M_{\text{ej},1}}{\lambda_1 R_1} + R_1^2 \left( \frac{T_1}{T_2} \right)^4 \right], \quad c = \frac{C' A M_2 M_{\text{ej}}}{\lambda_2},$$

with  $A \equiv G/4\pi\sigma T_2^4 t_{\text{inj}}$ . The relevant solution is

$$R_{2,\text{thm}} = 2\sqrt{-\frac{b}{3}} \cos \left[ \frac{1}{3} \arccos \left( \frac{3c}{2b} \sqrt{-\frac{3}{b}} \right) \right]. \quad (17)$$

If  $E_{\text{ej}} = 0$ , then  $c = 0$  and  $R_{2,\text{thm}} = \sqrt{-b}$ .

In the top panel of Fig. 2, we plot  $R_2/R_1$  against  $M_{\text{ej}}$  for four different models. All models assume  $\beta_1 = 0.9$ ,  $\lambda_1 = 1$ , and  $C' = \lambda_2$ . The solution can transition from  $R_{2,\text{max}}/R_1$  (steeper portion of the curves) to  $R_{2,\text{thm}}/R_1$  (flatter portion) when  $M_{\text{ej}}$  drops below some critical value. We consider our two example primary stars from Sec. 2.2. However, now the solution also depends on  $R_1$ , which we set to  $60 R_{\odot}$  ( $180 R_{\odot}$ ) for the  $1 M_{\odot}$  ( $3 M_{\odot}$ ) star, and  $\lambda_2$ , which we set to 1 (3), so that the ratio  $\lambda_2/\lambda_1 = 1$  (3) is preserved from those examples. In addition, we illustrate two different values of  $t_{\text{inj}}$ : 10 yr and 100 yr; these choices are motivated in Sec. 3.2. Finally, we adopt  $T_1 = T_2 = 4 \times 10^3$  K for each curve. We see that  $R_2/R_1 \sim 1.5\text{--}5$  if  $M_{\text{ej}} \lesssim 0.2 M_{\odot}$ .

In the bottom panel, we adopt  $M_{\text{ej}} = 0$ , i.e. zero mass loss during CE1, and  $t_{\text{inj}} = 10$  yr, and plot  $R_2/R_1$  against  $R_1$ , changing one parameter value at a time in each of the models shown. The solution changes from  $R_{2,\text{max}}/R_1$  (flat) to  $R_{2,\text{thm}}/R_1$  at some critical value of  $R_1$ . As in the top panel, all models assume  $\beta_1 = 0.9$ ,  $\lambda_1 = 1$ , and  $C' = \lambda_2$ . Reducing  $T_2$  reduces  $\Delta L_{\text{rad}}$ , which can increase  $R_2/R_1$ , so our choice of  $T_2 = T_1$  for most of the curves is conservative. The black (red) curve in the top and bottom panels corresponds to the same overall model, sliced through  $R_1 = 60 R_{\odot}$  ( $R_1 = 180 R_{\odot}$ ) in the top panel and  $M_{\text{ej}} = 0$  in the bottom.

### 3.2 Injection time scale

For the cases of Sec. 2.1, we estimate the duration of energy injection into the envelope,  $t_{\text{inj}}$ , motivating the values of Sec. 3.1. In case (i) the tidally disrupted planet is accreted onto the WD, liberating its orbital energy. If accretion sustains (Guidarelli et al. 2019), the Eddington rate is (e.g. Chamandy et al. 2018)  $\dot{M}_{\text{Edd}} \sim 2.7 \times 10^{-5} M_{\odot} \text{ yr}^{-1}$  ( $R_{\text{wd}}/0.013 R_{\odot}$ ), and

$$t_{\text{inj}} \sim \frac{m_1}{\dot{M}_{\text{Edd}}} \sim 4 \times 10^1 \text{ yr} \left( \frac{m_1}{10^{-3} M_{\odot}} \right) \left( \frac{R_{\text{wd}}}{0.013 R_{\odot}} \right)^{-1}. \quad (18)$$

But angular momentum redistribution during tidal disruption could swiftly drive some material to the core (Guidarelli et al., in preparation). For case (i), we thus crudely estimate  $1 \lesssim t_{\text{inj}} \lesssim 100$  yr. For case (ii), orbital energy is injected only down to the tidal disruption separation, and  $t_{\text{inj}}$  is smaller.

The envelope responds to energy injection on its sound-crossing time, of order of days to months. If the energy is deposited at the base of the convective zone, then convection transfers it to the envelope on a convective time, a few sound-crossing times. If energy is deposited in a deeper radiative zone, this delays the energy to the envelope by of order

a photon diffusion time  $\sim 10$  yr using Chamandy et al. (2019). The envelope would continue to adjust as this energy is transferred. These processes might stall the envelope response but are unlikely to change its duration. We have thus assumed in Sec. 3.1, that the envelope responds on a time  $\sim t_{\text{inj}}$ .

#### 4 CONCLUSIONS

Planets incurring successive CE events can combine to eject a stellar envelope. A planet interior to WD 1856 b could have partially unbound and expanded the envelope, which engulfed WD 1856 b and caused CE2, which completed the ejection and left the planet stabilized in its observed state. We find that  $0.2 \lesssim m_1/M_J \lesssim 30$  emerges as a plausible range for the mass of the planet/brown dwarf involved in CE1.

We estimated the stellar radius increase during CE1 using energy arguments, allowing for mass loss and radiative cooling, finding the ratio of final to initial radii  $1.5 \lesssim R_2/R_1 \lesssim 10$ . CE1 can thus plausibly initiate CE2. However, the envelope cannot expand if the ejecta carries away too much energy and offers too little drag on the secondary to compensate.

Since the orbit of planet 2 stabilizes around the time of CE2, our model predicts a more uniform distribution in WD ages than does the ZLK-tidal friction mechanism, which requires much longer time scales to operate. Our two-planet scenario could be generalized to more planets with only the final event ejecting the envelope and avoiding disruption. Massive planets are more likely to eject what remains so the last surviving planet would likely be relatively massive.

Evidence for previous mergers of planets with the stellar core in our scenario may be chemical enrichment of the WD, or accretion discs (e.g. Koester 2009; Girven et al. 2012; Doyle et al. 2019; Veras & Heng 2020), if sufficiently young, or high WD magnetic fields if the fields are acquired by accretion of a tidally disrupted companion (Nordhaus et al. 2011). Further work on the angular momentum distribution of WDs may be of interest in this context, as accretion can spin up the WD whilst magnetic braking can spin it down.

Our results are broadly consistent with Siess & Livio (1999a,b), who compute detailed spherically symmetric models involving a  $3M_\odot$  AGB star or  $\sim 1M_\odot$  RGB star undergoing accretion of planetary or brown dwarf material deep inside the envelope. A  $\sim 2$ -fold radial expansion of the star over  $\sim 100$  yr is fairly typical for their models, and in some cases accretion increases nuclear burning, resulting in a  $\sim 4$ -fold expansion over  $\sim 10$  yr. That the primary's envelope would expand significantly during a CE interaction with a planet is further supported by Staff et al. (2016), who simulated CE interactions between a  $10M_J$  planet and a  $3.5M_\odot$  RGB star or  $3.05M_\odot$  AGB star, finding that the envelope expands by  $\sim 40\%$  or  $\sim 20\%$ , respectively. Higher resolution simulations that can follow the inspiral down to smaller separations, and further release of orbital energy, would be desirable.

#### ACKNOWLEDGEMENTS

We acknowledge A. Frank for discussions, the referee for key suggestions, N. Soker for helpful comments, and US DOE grants DE-SC0001063, DE-SC0020432, DE-SC0020103; NSF grants AST-2009713, AST-1515648, AST-1813298, PHY-2020249; STSCI grant HST-AR-12832.01-A, HST-AR-15044.

#### DATA AVAILABILITY

Observational data are taken from Vanderburg et al. (2020).

#### References

- Chabrier G., 2003, *PASP*, **115**, 763  
 Chamandy L., et al., 2018, *MNRAS*, **480**, 1898  
 Chamandy L., Blackman E. G., Frank A., Carroll-Nellenback J., Zou Y., Tu Y., 2019, *MNRAS*, **490**, 3727  
 Chamandy L., Blackman E. G., Frank A., Carroll-Nellenback J., Tu Y., 2020, *MNRAS*, **495**, 4028  
 Chen Z., Blackman E. G., Nordhaus J., Frank A., Carroll-Nellenback J., 2018, *MNRAS*, **473**, 747  
 Clayton M., Podsiadlowski P., Ivanova N., Justham S., 2017, *MNRAS*, **470**, 1788  
 Cummings J. D., Kalirai J. S., Tremblay P. E., Ramirez-Ruiz E., Choi J., 2018, *ApJ*, **866**, 21  
 Debes J. H., Sigurdsson S., 2002, *ApJ*, **572**, 556  
 Doyle A. E., Young E. D., Klein B., Zuckerman B., Schlichting H. E., 2019, *Science*, **366**, 356  
 Fabrycky D., Tremaine S., 2007, *ApJ*, **669**, 1298  
 Gänsicke B. T., Schreiber M. R., Toloza O., Gentile Fusillo N. P., Koester D., Manser C. J., 2019, *Nature*, **576**, 61  
 Girven J., Brinkworth C. S., Farihi J., Gänsicke B. T., Hoard D. W., Marsh T. R., Koester D., 2012, *ApJ*, **749**, 154  
 Guidarelli G., Nordhaus J., Chamandy L., Chen Z., Blackman E. G., Frank A., Carroll-Nellenback J., Liu B., 2019, *MNRAS*, **490**, 1179  
 Hill G. W., 1886, *Acta Math.*, **8**, 1  
 Ivanova N., et al., 2013, *ARA&A*, **21**, 59  
 Koester D., 2009, *A&A*, **498**, 517  
 Kozai Y., 1962, *AJ*, **67**, 591  
 Lagos F., Schreiber M. R., Zorotovic M., Gänsicke B. T., Ronco M. P., Hamers A. S., 2021, *MNRAS*, **501**, 676  
 Lidov M. L., 1962, *Planet. Space Sci.*, **9**, 719  
 MacLeod M., Ostriker E. C., Stone J. M., 2018, *ApJ*, **863**, 5  
 Maldonado R. F., Villaver E., Mustill A. J., Chavez M., Bertone E., 2020, *MNRAS*, **497**, 4091  
 Meyer F., Meyer-Hofmeister E., 1979, *A&A*, **78**, 167  
 Muñoz D. J., Petrovich C., 2020, *ApJ*, **904**, L3  
 Nordhaus J., Blackman E. G., 2006, *MNRAS*, **370**, 2004  
 Nordhaus J., Spiegel D. S., 2013, *MNRAS*, **432**, 500  
 Nordhaus J., Spiegel D. S., Ibgui L., Goodman J., Burrows A., 2010, *MNRAS*, **408**, 631  
 Nordhaus J., Wellons S., Spiegel D. S., Metzger B. D., Blackman E. G., 2011, *PNAS*, **108**, 3135  
 O'Connor C. E., Liu B., Lai D., 2021, *MNRAS*, **501**, 507  
 Paxton B., et al., 2019, *ApJS*, **243**, 10  
 Siess L., Livio M., 1999a, *MNRAS*, **304**, 925  
 Siess L., Livio M., 1999b, *MNRAS*, **308**, 1133  
 Staff J. E., De Marco O., Wood P., Galaviz P., Passy J.-C., 2016, *MNRAS*, **458**, 832  
 Stephan A. P., Naoz S., Gaudi B. S., 2020, arXiv e-prints, p. arXiv:2010.10534  
 Vanderburg A., et al., 2020, *Nature*, **585**, 363  
 Veras D., Heng K., 2020, *MNRAS*, **496**, 2292  
 Veras D., Wyatt M. C., Mustill A. J., Bonsor A., Eldridge J. J., 2011, *MNRAS*, **417**, 2104  
 Villaver E., Livio M., 2009, *ApJ*, **705**, L81  
 Wilson E. C., Nordhaus J., 2019, *MNRAS*, **485**, 4492  
 Wilson E. C., Nordhaus J., 2020, *MNRAS*, **497**, 1895  
 Wu Y., Murray N., 2003, *ApJ*, **589**, 605  
 Xu X.-J., Li X.-D., 2010, *ApJ*, **716**, 114  
 von Zeipel H., 1910, *Astronomische Nachrichten*, **183**, 345